

## Dose Calculations for Lung Inhomogeneity in High-Energy Photon Beams and Small Beamlets: A Comparison between XiO and TiGRT Treatment Planning Systems and MCNPX Monte Carlo Code

Asghar Mesbahi<sup>1,2\*</sup>, Ismail Zergoug<sup>3</sup>

### Abstract

#### Introduction

Radiotherapy with small fields is used widely in newly developed techniques. Additionally, dose calculation accuracy of treatment planning systems in small fields plays a crucial role in treatment outcome. In the present study, dose calculation accuracy of two commercial treatment planning systems was evaluated against Monte Carlo method.

#### Materials and Methods

Siemens Once or linear accelerator was simulated, using MCNPX Monte Carlo code, according to manufacturer's instructions. Three analytical algorithms for dose calculation including full scatter convolution (FSC) in TiGRT, along with convolution and superposition in XiO system were evaluated for a small solid liver tumor. This solid tumor with a diameter of 1.8 cm was evaluated in a thorax phantom, and calculations were performed for different field sizes (1×1, 2×2, 3×3 and 4×4 cm<sup>2</sup>). The results obtained in these treatment planning systems were compared with calculations by MC method (regarded as the most reliable method).

#### Results

For FSC and convolution algorithm, comparison with MC calculations indicated dose overestimations of up to 120% and 25% inside the lung and tumor, respectively in 1×1 cm<sup>2</sup> field size, using an 18 MV photon beam. Regarding superposition, a close agreement was seen with MC simulation in all studied field sizes.

#### Conclusion

The obtained results showed that FSC and convolution algorithm significantly overestimated doses of the lung and solid tumor; therefore, significant errors could arise in treatment plans of lung region, thus affecting the treatment outcomes. Therefore, use of MC-based methods and super position is recommended for lung treatments, using small fields and beamlets.

**Keywords:** Convolution, Small Beamlet, Monte Carlo, Radiation Therapy, Treatment Planning.

---

*1-Department of Medical Physics, Medical School, Tabriz University of Medical Sciences, Tabriz, Iran.*

*2- Department of Radiation Oncology, Imam Hospital, Tabriz, Iran.*

*3-Department of Radiotherapy, Emir Abdelkader Anti-Cancer Center, Oran, Algeria*

\* Corresponding author: Tel: +98-9141193747, E-mail: [amesbahi2010@gmail.com](mailto:amesbahi2010@gmail.com),  
[mesbahiiiran@yahoo.com](mailto:mesbahiiiran@yahoo.com)

## 1. Introduction

Today, different small-radiation fields and beamlets are being utilized in newly developed techniques such as image-guided radiation therapy and stereotactic body radiation therapy for lung cancer treatment. In comparison with previously-established methods (e.g., three-dimensional conformal radiation therapy), application of these novel techniques has revealed promising results by tailoring the required dose distribution, based on the geometric spread of cancerous tissues, and preserving more healthy vital organs around tumors.[1].

Consequently, the importance and role of dose calculation algorithms for accurate dose estimations and obtaining the desired treatment outcomes have been accentuated. Dose calculations inside the lung have been resolved to some extent with the emergence of more complex and sophisticated algorithms in current treatment planning systems (TPSs), especially with the application of Monte Carlo (MC) methods in some commercial dose calculation systems [1-4]. On the other hand, other algorithms with reliable results have been installed in newly developed systems, showing high applicability in radiation therapy planning calculations.[5-7].

Several studies on dose calculation accuracy for small fields have shown that use of TPSs, along with correction-based methods, may provide inaccurate results, compared to MC measurements [5-16]. On the other hand, recent algorithms such as collapsed cone convolution and analytical anisotropic algorithm (AAA) have presented reliable and accurate results for small beamlets, used in lung treatments[17]. The results obtained in electronic disequilibrium conditions were comparable to MC simulations and measurements. However, the accuracy of newly developed TPSs should be verified for such extreme dose calculations before clinical application.

The main objective of this study was to compare the performance of two newly installed TPSs, i.e., XiO and TiGRT, with MC calculations by MCNPX code. It should be noted that TiGRT system has been recently

employed in Iran, providing three-dimensional conformal radiotherapy and intensity-modulated radiation therapy (IMRT) calculations.

Unfortunately, in the literature, no previous study has evaluated the accuracy of this TPS in terms of performance, using IMRT beams. In the current study, calculations were performed on a thorax phantom, consisting of a lung with a small solid tumor. Dose variations within the lung and tumor on the central axis of the beam were calculated by the MC method and three introduced algorithms.

## 2. Materials and Methods

### 2.1. TiGR TTPS

TiGRT was designed by Lina Tech (Sunnyvale, CA, USA) for dose calculations in external photon and electron beams. This system is able to support all commercial linear accelerators with different multi-leaf collimators (MLCs), as well as step-and-shoot and dynamic IMRT methods. Moreover, for dose calculations in patients, TiGRT applies X-ray computed tomography images. Also, this system is capable of integrating other imaging modalities including magnetic resonance imaging, single-photon emission computed tomography, positron emission imaging and X-ray computed tomography for efficient treatment planning. (TiGRT user manual).

According to user's manual, TiGRT system uses an exclusive algorithm, known as full scatter convolution (FSC), developed to facilitate fast and accurate calculations. This algorithm uses basic beam data, collected during device commissioning including tissue maximum ratio, beam profile, total scatter factors and collimator parameters.

Dose calculation time is under ten seconds per beam for conventional and three-dimensional conformal techniques. An overall accuracy of more than 3% has been reported by the user's manual. According to this manual, FSC algorithm separates the absorbed dose  $D$  in a given point into the primary dose  $D_p$  and the scatter dose  $D_s$ :

$$D = D_p + D_s \quad (1)$$

The primary dose  $D_p(\vec{r})$  is calculated based on the convolution algorithm, using the following formula:

$$D_p(\vec{r}) = \iiint \Phi_p(\vec{r}') k_p(\vec{r} - \vec{r}') dV' \quad (2)$$

where  $\Phi_p(\vec{r}')$  denotes photon fluence at the surface of a ray passing through the surface to point  $\vec{r}'$  and  $k_p(\vec{r} - \vec{r}')$  is the electron transport kernel, describing the dose distribution around the primary interaction site of the photon. This shows that the electron transport modeling has been taken into account by this algorithm, and the electron dose deposition kernel can be scaled for in homogeneities such as bone, lung and air cavities. Finally,  $dV'$  is the differential calculation volume at point  $\vec{r}'$ .

The scatter dose  $D_s(\vec{r})$  is derived from the following convolution equation:

$$D_s(\vec{r}) = \iiint \Phi_p(\vec{r}') k_s(\vec{r} - \vec{r}') dV' \quad (3)$$

In this algorithm, multiple scattering of photons is discarded and  $k_s(\vec{r} - \vec{r}')$  is the first scatter fluence kernel. This kernel can be derived from the electron transport kernel. For more detailed explanations, readers can refer to the user's manual of this TPS.

### 2.2. XiO TPS

XiO TPS (Elekta, Stockholm, Sweden) employs fast-Fourier transform (FFT) convolution and multi-grid superposition algorithms. These two algorithms are similar as they both perform dose calculations by convolving the total energy released in patients by MC-generated energy deposition kernels. However, the major difference between these two algorithms is that FFT convolution does not calculate the dose as accurately as multi-grid superposition in the presence of tissue in homogeneities. In this study, for simplicity, we applied convolution and superposition terms instead of FFT convolution and multi-grid superposition, respectively.

Tissue in homogeneities cause considerable changes in the shape of energy deposition kernels and the resultant dose distribution in comparison with predictions in homogenous water-like content. Therefore, an important

factor in accurate dose calculations is to account for tissue in homogeneities in newly developed algorithms. In both XiO algorithms, tissue, which is located along the primary radiation ray lines, directly influences dose deposition kernels at each point in patients.

Unlike FFT convolution algorithm, in multi-grid superposition, energy deposition kernels are modified to account for variations in electron density in different types of tissues. The density scaling method is used to distort the kernels by determining the average density along the straight-line path between the interaction site and dose deposition site.

Convolution and superposition dose calculation algorithms used in XiO TPS are briefly described here. Dose at point  $\vec{r}$  is calculated as the sum of total energy released per unit mass at point  $T(\vec{r}')$ , multiplied by the value of the energy deposition kernel  $H(\vec{r} - \vec{r}')$  that is, originated at point  $r'$  and evaluated at point  $r$ .

Two equations used for convolution and superposition algorithms are as follows:

$$(1) \quad D(\vec{r}) = \int T(\vec{r}') H(\vec{r} - \vec{r}') d^3r' \text{ for FFT convolution}$$

$$(2) \quad D(\vec{r}) = \int T(\vec{r}') \frac{\rho(r')}{\bar{\rho}} K_p(\bar{\rho}|\vec{r} - \vec{r}'|, \vec{r} - \vec{r}') d^3r' \text{ for superposition}$$

In these equations,  $D(\vec{r})$  denotes the dose at the given point  $\vec{r}$ ,  $\rho(r')$  is the density of material at photon interaction point and  $\bar{\rho}$  is the average density along the straight-line path between the interaction point and dose deposition site. For more detailed explanation about the algorithms, reading the user's manual of XiO TPS is recommended.

### 2.3. MC simulations

The head of Siemens oncor impression was simulated by MCNPX code (2.4.1)[18]. The model consisted of an electron target, primary collimator, flattening filter and secondary collimators, according to manufacturer's instructions (Figure 1). An MLC (41 pairs) was the secondary collimator jaw in X-axis and the width of the leafs at the isocenter was 1 cm. However, to avoid difficulties related to the complexity of inter-leaf leakage and beam validation, MLC was not simulated in our

model; MLC simulation was performed similar to Y-axis secondary collimator jaws.

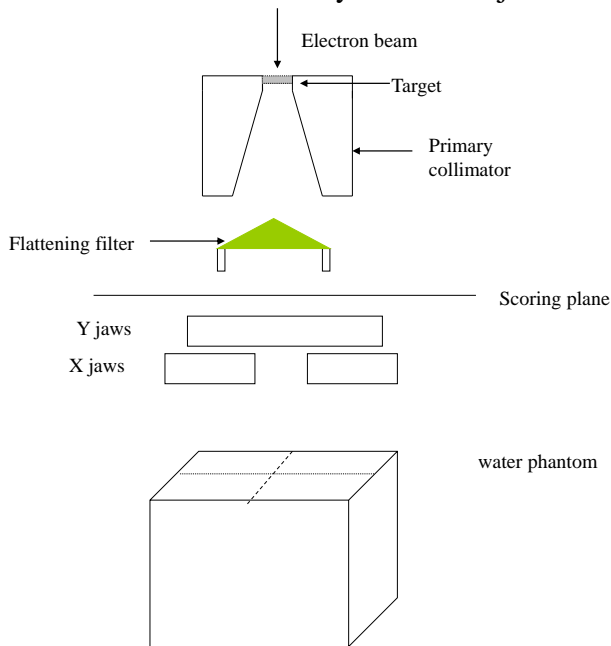


Figure 1. The schematic geometry of Monte Carlo model of Oncor Linac head

For MC dose calculations inside the phantom, a phase space (PS) file (about 10 GB) was generated by scoring the particles crossing a plane just above the secondary collimators for the evaluated energies. Then, the PS file was used for the second part of depth dose calculations. In the second part, the PS file was used as a photon source. Only the opening of the secondary collimator was changed to provide the field sizes for further calculations. For model validation, the percentage depth doses and beam profiles for  $5 \times 5$ ,  $10 \times 10$  and  $20 \times 20$  cm<sup>2</sup> field sizes were calculated by the MC model and compared with water phantom measurements [11-14]. The primary electron energy was set to 6.1 MeV and 18 MeV after tuning by comparing the measured and calculated percentage depth dose (PDD) curves in  $10 \times 10$  cm<sup>2</sup> field size.

The comparison of calculated PDDs in the water phantom for  $5 \times 5$  and  $10 \times 10$  cm<sup>2</sup> field sizes is presented in figures 2 and 3. The measured PDDs and beam profiles of both photon beams, used as the basic beam data for TPS installation, were applied for MC model validation. It should be noted that the beam

profile comparison was not demonstrated in the present study due to limitations in the number of figures.

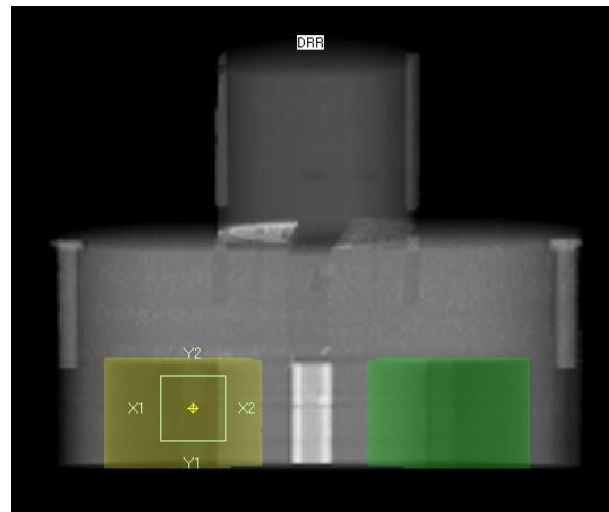


Figure 2. Thorax phantom geometry and the designed solid tumor inside the lung: (A) an X-ray computed tomography slice, (B) a digitally reconstructed radiograph from the thorax phantom

For depth dose calculations in the water and inhomogeneous lung phantom, a column of scoring cells with a dimension of  $2 \times 2 \times 2$  mm<sup>3</sup> was defined in the central axis of the beam, using the lattice command in MCNPX code. Dose deposition was scored by \*F8 energy deposition tally, which scores the deposited energy inside the cells in terms of MeV. The thorax phantom was modeled geometrically in the MC input file, using actual dimensions and material properties of the used thorax phantom.

For depth dose calculations inside the lung phantom, the calculated values in terms of MeV were changed to MeV/g and PDD was then calculated. Photon and electron energy cut-off points of 0.5 and 0.01 KeV were used for MC simulations, respectively. MC runs were performed on a desktop computer and statistical uncertainty of results was less than 2% for all MC calculations.

### 3. Results

The results of MC modeling for the Linac head are presented in figures 3 and 4 for 6 and 18 MV photon beams. In these figures, PDD curves for different field sizes ( $5 \times 5$  and  $10 \times 10$

## Dose Calculations for lung Inhomogeneity in Small Beamlets

cm<sup>2</sup>) were compared with the measured depth doses in the water phantom. The measurements obtained from the

commissioning data were used in the department of radiation therapy for dose calculations as the basic beam data.

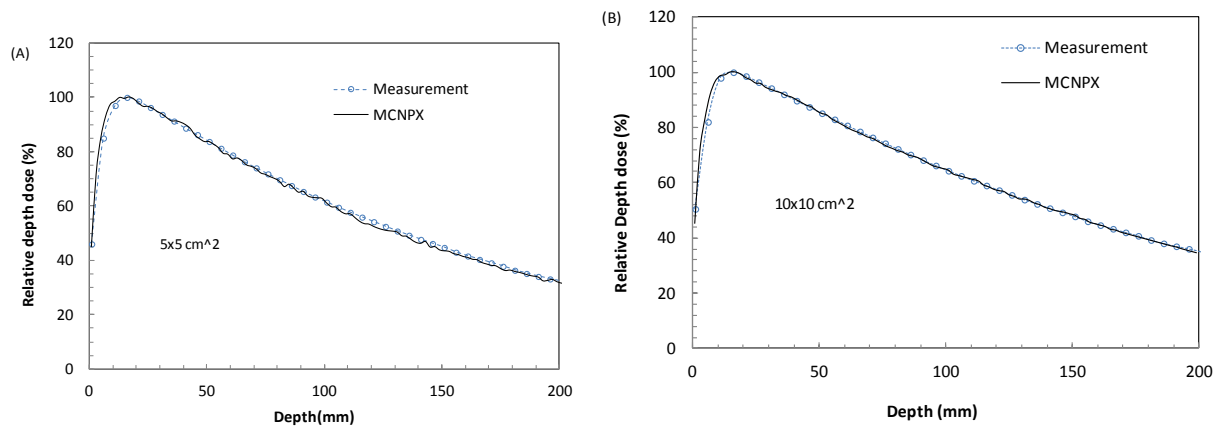


Figure 3. The comparison of relative depth doses calculated by Monte Carlo method and measurements in a homogenous water phantom for two field sizes: (A) 5×5 cm<sup>2</sup> and (B) 10×10 cm<sup>2</sup> for the 6 MV photon beam

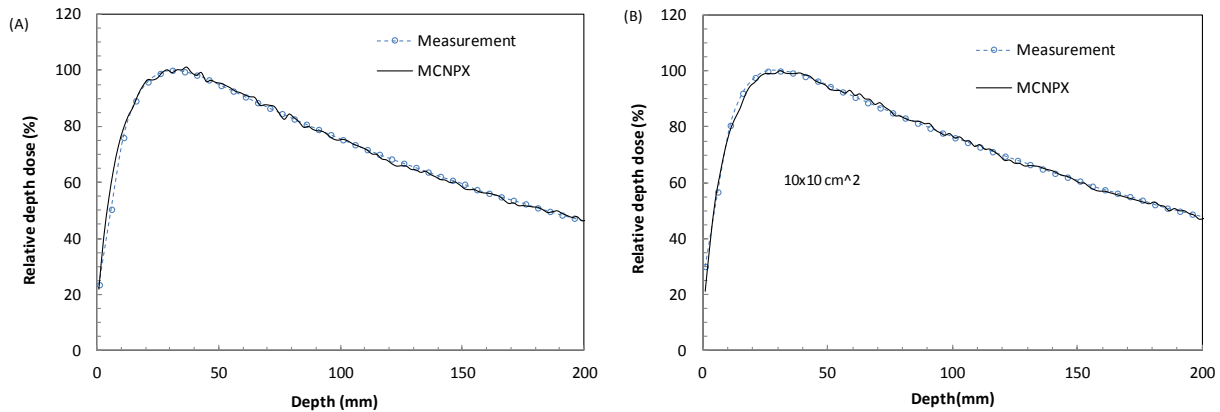


Figure 4. The comparison of relative depth doses obtained by measurements and Monte Carlo method in a homogenous water phantom for two field sizes: (A) 5×5cm<sup>2</sup> and (B) 10×10 cm<sup>2</sup> for the 18 MV photon beam

The differences between the MC calculated and measured depth dose curves were evaluated for build-up and descending parts. For the build-up region, a difference of up to 10% was seen due to inaccuracies in ionization chamber measurements in this region, as reported by previous studies[11-13,19,20]. For the descending part of all depth dose curves, the discrepancy between MC results and the measurements was found to be less than 2% for all energies and field sizes. The beam profiles at the depth of 10 cm were also calculated for different field sizes (from 5×5 cm<sup>2</sup> to 20×20 cm<sup>2</sup>) to validate our MC model. For profiles, the difference between MC calculations and measurement results was less

than 3% inside the beam. Consequently, our MC model was validated by comparing MC calculations and measurement results. As these findings were not in line with the purpose of this study, they were discarded.

To evaluate the accuracy of TiGRT and XiO TPSs for small beamlets (used for the treatment of a solid tumor inside the lung), depth doses along the central axis of the beam were calculated via four methods: MC, FSC, convolution and superposition algorithms. The results of depth dose calculations along the central axis of inhomogeneous lung phantom are presented in figures 5 and 6 for 6 and 18 MV photon beams, respectively.

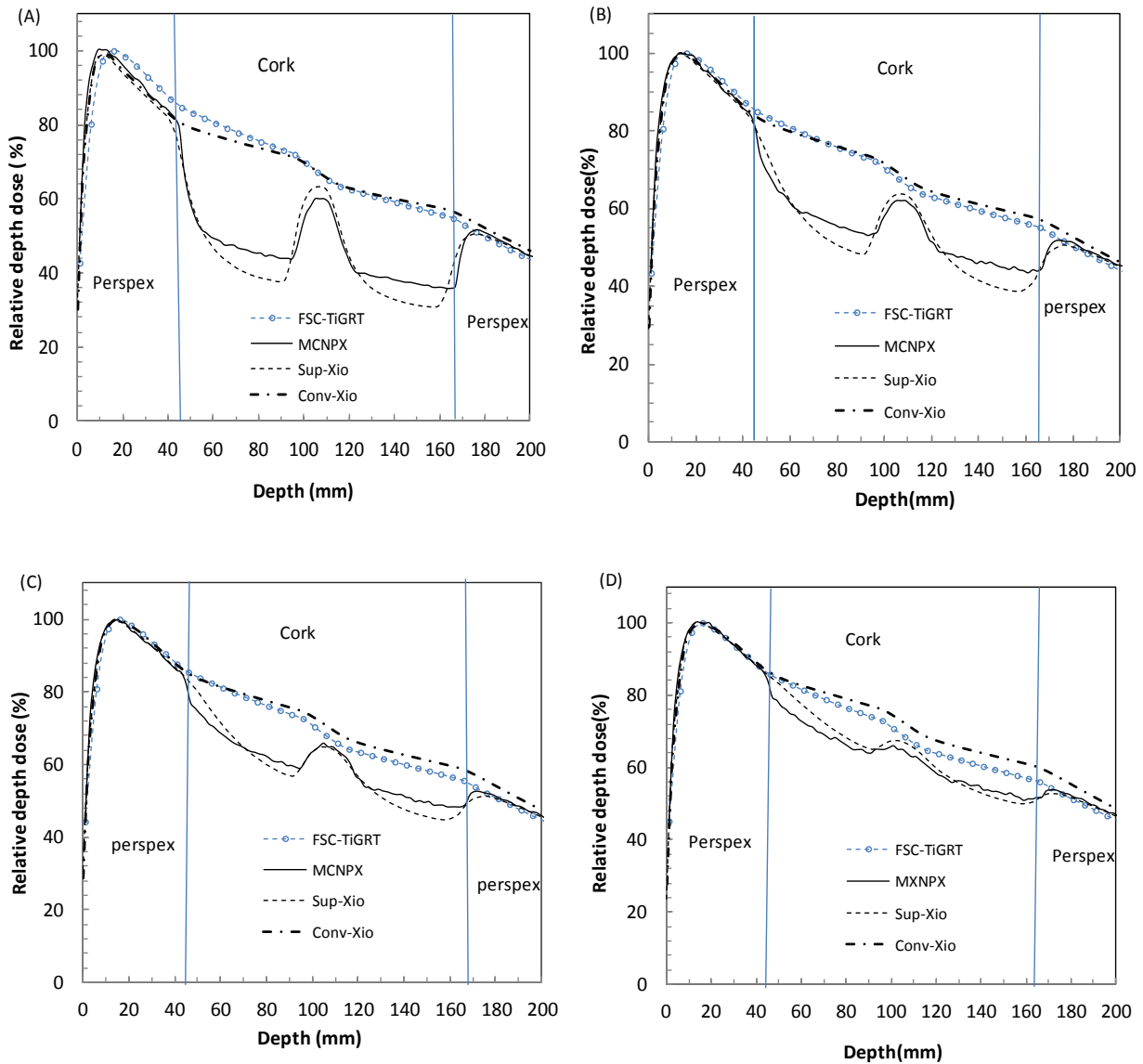


Figure 5: Depth dose comparison among four calculation methods for the 6 MV photon beam in different field sizes: A) 1x1 cm<sup>2</sup>, B) 2x2 cm<sup>2</sup>, C) 3x3 cm<sup>2</sup>, D) 4x4 cm<sup>2</sup>

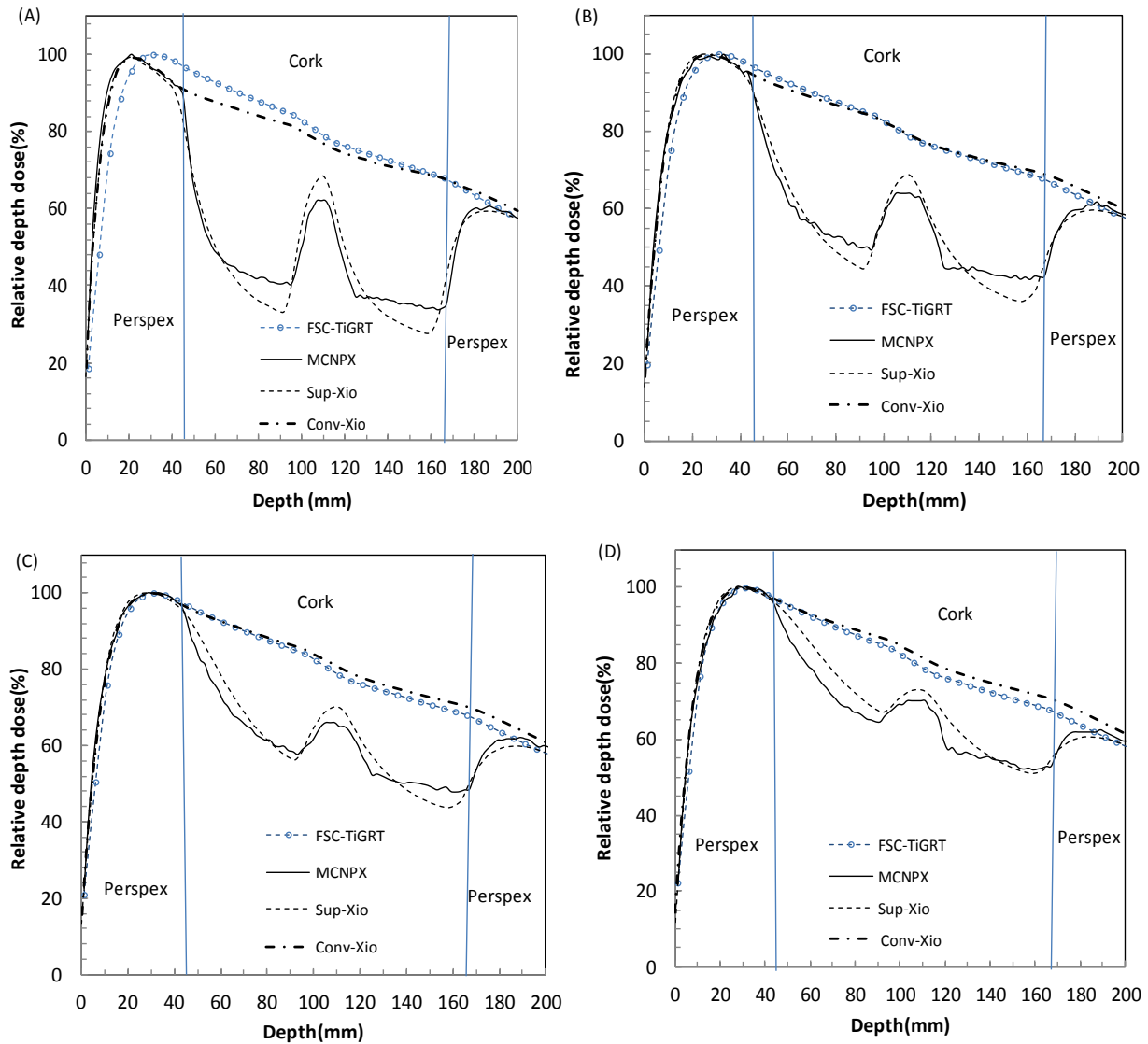


Figure 6: Depth dose comparison among four calculation methods for the 18 MV photon beam in different field sizes: A)  $1 \times 1 \text{ cm}^2$ , B)  $2 \times 2 \text{ cm}^2$ , C)  $3 \times 3 \text{ cm}^2$ , D)  $4 \times 4 \text{ cm}^2$

#### 4. Discussion

As presented in figures 5 and 6, the dose build-up and build-down regions were pronounced in smaller field sizes. The most extreme dose reduction in the lung region was reported in the field size of  $1 \times 1 \text{ cm}^2$ , while in the field size of  $4 \times 4 \text{ cm}^2$ , dose variations in the lung and tumor were not considerable.

Comparison of different algorithms showed that FSC and convolution could predict depth doses in a similar pattern in different regions,

e.g., lung-unit density interfaces and inside the lung. Among the evaluated TPSs, XiO superposition calculated dose variations, similar to MC method and showed a very close agreement with MC results in all regions, in spite of slight discrepancies in some regions, particularly in lung-unit density interfaces. For the 18 MV photon beam (Figure 6), the effect of electronic disequilibrium became more pronounced, since the higher range of secondary electrons produced inside the lung led to a greater dose reduction inside the lung

and increased the observed depth fall-off inside the lung, compared to 6 MV photon beam. Neither FSC nor the convolution algorithm was able to account for the effect of secondary electron equilibrium inside the lung or lung-unit density interfaces. This is due to the fact that these models do not accurately consider the secondary electron transport in the low-density region.

Comparison of MC results and superposition algorithm showed that both methods could account for the electronic disequilibrium inside the lung, considering the dose fall-off caused by the absence of secondary electrons inside the lung and solid tumor; however, the discrepancy between these two methods cannot be ignored. As it can be seen, the superposition algorithm could better estimate lower doses for the points inside the lung, compared to the MC method. On the other hand, the steepness of dose build-up and build-down curves in these two methods differed moderately in both energies.

The results of FSC and convolution algorithm were inconsistent with MC and superposition findings in  $1 \times 1 \text{ cm}^2$  field size for both energies. However, in larger field sizes, the discrepancy reduced considerably, while the effect of electronic equilibrium was minimized. As the comparison of convolution algorithm and FSC indicated, they could calculate the depth dose in a similar pattern along the central axis, regardless of lung and unit density materials.

However, there were small differences between the algorithms in the  $1 \times 1 \text{ cm}^2$  field size for both energies. It should be mentioned that the tumor dose was also overestimated up to 25% by FSC and convolution method in the middle of the tumor in all field sizes and energies. Additionally, these methods overestimated the lung dose up to 120% in the

field size of  $1 \times 1 \text{ cm}^2$  with 18 MV energy. The extent of overestimation reduced by increasing the field size and lowering the energy; it reached to 80% and 38% for  $2 \times 2$  and  $4 \times 4 \text{ cm}^2$  field sizes, respectively.

In a similar study by Carrasco *et al.*, evaluating dose calculation algorithms and their accuracy, the dose inside a heterogeneous lung-like phantom was measured for small field sizes ( $2 \times 2$  and  $1 \times 1 \text{ cm}^2$ ) [21]. The performance of four correction-based algorithms and one based on convolution-superposition was studied. The correction-based algorithms included Batho, modified Batho, and TAR implemented in Cadplan TPS (Varian) and Helax-TMS Pencil Beam.

In the mentioned study, the convolution-superposition algorithm was the collapsed cone, implemented in the Helax TMS. Among all evaluated methods, only the collapsed cone and MC results were in agreement with measurements within 2%. The largest difference (39%) between the predicted and delivered doses in the beam axis was observed in the EqTAR algorithm inside the lung-equivalent material in a  $2 \times 2 \text{ cm}^2$  field size with an 18 MV X-ray beam.

Chen *et al.* compared X-ray voxel-based MC (XVMC) calculations and Pencil Beam measurements for lung lesions in terms of dose distribution in clinically applied non-intensity-modulated radiotherapy (15-MV plans) for stereotactic body radiotherapy [22]. The XVMC calculations agreed well with film measurements (<1% difference in the lateral profile), whereas the deviation between Pencil Beam calculations and film measurements was up to more than 15%.

In the mentioned study, the largest differences were observed for small lesions circumferentially encompassed by the lung

tissue. It was concluded that Pencil Beam dose calculations overestimate the dose to the tumor and underestimate lung volumes for the 15 MV photon beam.

Comparisons with MC calculations showed that the AAA algorithm provides the best simulations of depth dose curves in all investigated field sizes [5]. However, even this algorithm could not accurately predict depth dose values in the lung for field sizes of  $1 \times 1$  and  $2 \times 2$  cm<sup>2</sup>. Lung over doses of about 40% and 20% were calculated by the AAA algorithm close to the interface soft tissue/lung for  $1 \times 1$  and  $2 \times 2$  cm<sup>2</sup> field sizes, respectively. As the results indicated, 100% difference may be found between MC results and Batho, the modified Batho and equivalent TAR responses inside the lung for the  $1 \times 1$  cm<sup>2</sup> field size; this finding was quite similar to the current results for this field size.

It is worth mentioning that dose measurements in small fields need to be precisely aligned with a small detector; this process can be time-consuming and susceptible to several errors. Additionally, if we consider problems of lateral electronic equilibrium and tissue inhomogeneity, accurate dose determination may not be highly feasible by the measurements. However, MC method takes all these conditions into account in small-field dosimetry by transporting the secondary electrons inside inhomogeneity and simulating the electronic disequilibrium in all dose calculations.

With regard to the performance of superposition and MC methods, they were capable of predicting the dose drop-off in lung regions and tumor. Besides, both build-up and build-down regions could be accurately predicted by the MC method, which provided the most reliable results; it should be

mentioned that measurements for these regions, as well as lung-unit density interface, were not available in our study.

On the other hand, there was a slight difference between MC calculations and superposition algorithm inside the lung, as well as the build-up and build-down regions in terms of dose variation steepness. The dose gradient for superposition was slightly steeper than MC in all cases, leading to a dose underestimation of up to 25% in the worst condition, relative to MC calculations inside the lung for 18 MV energy.

## 5. Conclusion

In the current study, the performance of two commercial TPSs for dose calculations inside the lung, containing a solid tumor, was evaluated for small beamlets. The MC results were regarded as the most reliable for comparisons. FSC and convolution algorithms could not accurately estimate the dose inside the lung and solid tumor, compared to the MC method. On the other hand, the superposition algorithm of XiO TPS accurately predicted the dose distribution inside the lung and tumor; also, the effect of electronic disequilibrium in small fields was taken into account in this method. Findings of this study recommend the application of superposition algorithm for dose calculations in the lung region for small beamlets and beams instead of simple, inaccurate methods such as FSC and convolution methods.

## Acknowledgment

The authors would like to thank Dr. Behnam Nasiri, the head of radiation oncology department, Tabriz international hospital for his support.

## References

1. Rassiah- Szegedi P, Salter BJ, Fuller CD, Blough M, Papanikolaou N, Fuss M. Monte Carlo characterization of target doses in stereotactic body radiation therapy (SBRT). *Acta Oncologica*. 2006;45(7):989-94.
2. Scholz C, Nill S, Oelfke U. Comparison of IMRT optimization based on a pencil beam and a superposition algorithm. *Med Phys*.2003;30(7):1909-13.
3. Schwarz M, Alber M, Lebesque JV, Mijneer BJ, Damen EM. Dose heterogeneity in the target volume and intensity-modulated radiotherapy to escalate the dose in the treatment of non-small-cell lung cancer. *Int J Radiat Oncol Biol Phys*.2005; 62(2):561-70.
4. Seco J, Sharp GC, Wu Z, Gierga D, Buettner F, Paganetti H. Dosimetric impact of motion in free-breathing and gated lung radiotherapy: a 4D Monte Carlo study of intrafraction and interfraction effects. *Med Phys*.2008;35(1):356-66.
5. da Rosa LA, Cardoso SC, Campos LT, Alves VG, Batista DV, Facure A. Percentage depth dose evaluation in heterogeneous media using thermoluminescent dosimetry. *J Appl Clin Med Phys*.2010;11(1):2947.
6. Disher B, Hajdok G, Gaede S, Battista JJ. An in-depth Monte Carlo study of lateral electron disequilibrium for small fields in ultra-low density lung: implications for modern radiation therapy. *Phys Med Biol*.2012;57(6):1543-59.
7. Fotina I, Kragl G, Kroupa B, Trausmuth R, Georg D. Clinical comparison of dose calculation using the enhanced collapsed cone algorithm vs. a new Monte Carlo algorithm. *Strahlenther Onkol*.2011;187(7):433-41.
8. Fragoso M, Wen N, Kumar S, Liu D, Ryu S, Movsas B, Munther A, Chetty IJ. Dosimetric verification and clinical evaluation of a new commercially available Monte Carlo-based dose algorithm for application in stereotactic body radiation therapy (SBRT) treatment planning. *Phys Med Biol*.2010;55(16):4445-64.
9. Gagne IM, Zavgorodni S. Evaluation of the analytical anisotropic algorithm in an extreme water-lung interface phantom using Monte Carlo dose calculations. *J Appl Clin Med Phys*.2006;8(1):33-46.
10. Haedinger U, Krieger T, Flentje M, Wulf J. Influence of calculation model on dose distribution in stereotactic radiotherapy for pulmonary targets. *Int J Radiat Oncol Biol Phys*.2005;61(1):239-249.
11. Mesbahi A, Allahverdi M, Gheraati H, Mohammadi E. Experimental evaluation of ALFARD treatment planning system for 6 MV photon irradiation: A lung case study. *Rep Pract Oncol Radiother*.2004;9(6):217-21.
12. Mesbahi A, Allahverdi M, Gheraati H. Monte Carlo dose calculations in conventional thorax fields for <sup>60</sup>Co photons. *Radiat Med*.2005;23(5):341-50.
13. Mesbahi A, Thwaites DI, Reilly AJ. Experimental and Monte Carlo evaluation of Eclipse treatment planning system for lung dose calculations. *Rep Pract Oncol Radiother*.2006;11(3):123-33.
14. Mesbahi A. The effect of electronic disequilibrium on the received dose by lung in small fields with photon beams: Measurements and Monte Carlo study. *Iran J Radiat Res*.2008;6(2):71-77.
15. Motomura AR, Bazalova M, Zhou H, Keall PJ, Graves EE. Investigation of the effects of treatment planning variables in small animal radiotherapy dose distributions. *Med Phys*.2010;37(2):590-599.
16. Nakaguchi Y, Araki F, Maruyama M, Fukuda S. Comparison of RTPS and Monte Carlo dose distributions in heterogeneous phantoms for photon beams. *Nihon Hoshasen Gijutsu Gakkai Zasshi*.2010;66:322-33.

## Dose Calculations for lung Inhomogeneity in Small Beamlets

17. Sterpin E, Tomsej M, De SB, Reynaert N, Vynckier S Monte carlo evaluation of the AAA treatment planning algorithm in a heterogeneous multilayer phantom and IMRT clinical treatments for an Elekta SL25 linear accelerator. *Med Phys.*2007;34(5):1665-77.
18. Waters L. *MCNPX<sup>TM</sup> user's manual version 2.4.0*. Alamos: Los Alamos National Laboratory; 2002. Sep, Report No: LA-CP-02-408...
19. Mesbahi A, Fix M, Allahverdi M, Grein E, Garaati H. Monte Carlo calculation of Varian 2300C/D Linac photon beam characteristics: A comparison between MCNP4C, GEANT3 and measurements. *Appl Radiat Isot.*2005;62(3):469-77.
20. Mesbahi A, Reilly AJ, Thwaites DI. Development and commissioning of a Monte Carlo photon beam model for Varian Clinac 2100EX linear accelerator. *Appl Radiat Isot.*2006;64(6):656-62.
21. Carrasco P, Jornet N, Duch MA, Weber L, Ginjaume M, Eudaldo T, et al. Comparison of dose calculation algorithms in phantoms with lung equivalent heterogeneities under conditions of lateral electronic disequilibrium. *Med Phys.*2004;31(10):2899-911.
22. Chen H, Lohr F, Fritz P, Wenz F, Dobler B, Lorenz F, et al. Stereotactic, single-dose irradiation of lung tumors: a comparison of absolute dose and dose distribution between pencil beam and Monte Carlo algorithms based on actual patient CT scans. *Int J Radiat Oncol Biol Phys.*2010; 78(3):955-63.